Rev.Adv.Mater.Sci. 9 (2005) 17-33

ELASTIC FIELDS OF INCLUSIONS IN NANOCOMPOSITE SOLIDS

I.A. Ovid'ko and A.G. Sheinerman

Institute of Problems of Mechanical Engineering, Russian Academy of Sciences, Bolshoj 61, Vasil. Ostrov, St. Petersburg 199178, Russia

Reveived: February 17, 2005

Abstract. We give a brief overview of the analytical solutions for the elastic fields of inclusions in composite solids with an emphasis placed on nanocomposites. Besides, we describe the most popular analytical procedures used in calculations of the elastic fields of inclusions in nanocomposites. These procedures include the Green function method, the method of surface dislocation loops, integration of the equations of equilibrium, and the method of infinitesimal inclusions. Also, we discuss and compare the solutions for the elastic fields of nanoinclusions, derived within linear elasticity, with those obtained using atomistic simulations. With this comparison, it is shown that the linear elasticity approach is valid down to extremely small inclusion dimensions.

1. INTRODUCTION

Nanocomposite solids represent a wide class of solid composite materials consisting of at least one component with dimensions in the nanometer (1 nm = 10^{-9} m) range. These advanced materials have become increasingly important both in fundamental and applied research because of their unique mechanical, electronic and optical properties [1-4]. For example, nanocomposites may have higher strength and hardness, higher thermal stability and better electrical conductivity than their conventional counterparts. Of special importance are both nanotube-reinforced composites [5] and nanocomposites with ensembles of quantum dots and wires, which have unique optoelectronic properties [6-9].

The outstanding mechanical and electronic properties of nanocomposite solids are dramatically influenced by elastic fields of their inclusions. The knowledge of the elastic strains and stresses existing in nanocomposites is necessary in calculation of their mechanical strength, determination of the conditions for their fracture, and computation of the critical parameters for the formation of linear defects in nanocomposites. In the case of quantum dots and wires, their elastic fields crucially affect their electronic properties and influence the spatial arrangement, size and shape of the self-assembled nanostructures growing on the surface of a nanocomposite solid with quantum dots or wires.

The elastic fields acting in nanocomposite solids depend on a number of factors, which include material and geometric parameters of nanocomposites (types and parameters of the inclusion and matrix crystal lattices, inclusion size and shape, surface energy of the matrix-inclusion interface), and mutual diffusion of the matrix and inclusion.

In the nanocomposites having the structure of a solid solution, their elastic fields may also be influenced by the segregation of the atoms of the same kind. In spite of an essential mutual diffusion of the matrix and inclusions in nanocomposites [10-21],

Corresponding author: I.A. Ovid'ko, e-mail: ovidko@def.ipme.ru

the calculation of the elastic fields, acting in nanocomposites, with an account of a real spatially inhomogeneous concentration distribution of different components is a very complicated problem. Therefore, for the calculation of elastic fields of nanoscopic inclusions, atomic diffusion is commonly neglected.

The elastic fields acting in nanocomposites are computed using different approaches. These approaches include the methods of classical linear elasticity [22-47], atomistic calculations [26,39,48-57], and the methods that combine elastic continuum models of nanocomposites with atomistic calculations (e.g., [58]). In the continuum models based on the elasticity theory, inclusions in nanocomposites are described using the tensor of eigenstrains, which are associated with the difference (misfit) of the matrix and inclusion crystal lattices. Within the continuum approaches, the elastic fields acting in nanocomposites are calculated using analytical methods [22,23,25,27–29,34–37,41,43,47], or numerical techniques (finite element method [22,24,30,32,33,38,39,42,44–46], boundary integral method (e.g., [40]), finite difference method (e.g., [26]), etc.).

In contrast to atomistic calculations, the use of continuum models for the calculation of inclusion elastic fields in nanocomposites allows one to obtain the solutions applicable for nanocomposites with different chemical composition. At the same time, classical linear elasticity may give inaccurate values of the inclusion elastic fields in the cases where the inclusion is facetted, its sizes are very small, or the misfit of the crystal lattice parameters of the matrix and inclusion is very high.

In the case of a facetted inclusion, the application of linear elasticity may lead to inexact values of inclusion elastic fields due to the singularity of some strain tensor components at the facetted inclusion edges. Therefore, in the regions near the inclusion edges, the linear elasticity theory is inapplicable. However, the sizes of these regions are very small, and so their existence is not essential.

In the case of a very small inclusion, the linear elasticity theory may fail when the smallest of the inclusion sizes is comparable to the size of an atom. To estimate the lower limit where linear elasticity is still valid, the elastic fields obtained in its frame should be compared to the results of atomistic calculations. Such a comparison has recently been carried out for spherical inclusions by Makeev *et al.* [54]. They have shown that the inclusion strains calculated within the two approaches coincide, if the inclusion radius exceeds 5 interatomic distances, and have small discrepancies for the inclusion radius of 4-5 interatomic distances. A perfect coincidence of the elastic fields of nanoscopic inclusions with different shapes, calculated within the continuum and atomistic approaches, has also been demonstrated in Refs. [38,50]. A discrepancy in the results provided by the continuum and atomistic calculations arises only in the case of a very high misfit between the matrix and inclusion crystal lattice parameters [26] and is, apparently, associated with the errors given by the linear elasticity theory at high strains.

Thus, the comparison of the results obtained within linear elasticity with atomistic calculations testifies to the opportunity of using the linear elasticity theory for the calculation of the elastic fields acting in nanocomposites. A brief review of the available analytical solutions for the elastic fields of nanocomposites will be given in the next section. In the following sections, we will also describe the most popular analytical techniques that allow one to calculate the displacement, strain and stress fields in nanocomposites.

2. ANALYTICAL SOLUTIONS FOR ELASTIC FIELDS OF INCLUSIONS

Consider a domain in a solid (nano)composite, which, in addition to elastic strains, is subjected to the action of inelastic strains (eigenstrains). Such inelastic strains may appear as a result of thermal expansion or contraction, arise due to the misfit of the crystal lattice parameters of the matrix and inclusion or originate in the course of phase transitions or plastic deformation. Following Mura [59], we will call such a domain an inclusion if its elastic constants are equal to the elastic constants of the rest of the material (matrix), and an inhomogeneity if its elastic constants differ from the elastic constants of the matrix. In the following, we will mainly consider the simpler case where the difference between the elastic constants of the different phases of the composite is not very large and the domain with an eigenstrain may be modeled as an inclusion.

The exact analytical solutions for the elastic fields of inclusions are available for isotropic and anisotropic inclusions situated in an infinite or semi-infinite medium, finite-thickness plate, cylinder, infinite plane or semiplane. First, examine the papers that address elastic fields of isotropic inclusions in an infinite medium. One of the pioneering works in this area is the work by Goodier [60]. In this work, the eigenstrains arose due to the thermal expansion, and elliptic and rectangular inclusions in a thin infi-

nite plate were considered. More recently, Miklestad [61] and Edward [62] examined the problems about the thermal stresses induced by an ellipsoidal inclusion and uniformly heated semi-infinite circular cylindrical inclusion. The solution for an ellipsoidal inclusion with arbitrary eigenstrains in an isotropic infinite medium was originally obtained in the works by Eshelby [63-65], which were later collected in book [66]. Eshelby, in particular, showed that elastic strains and stresses were uniform inside an ellipsoidal inclusion situated in infinite medium. The partial cases of an ellipsoidal inclusion are the cylindrical and spherical ones. The expressions for the elastic fields of an elastic cylindrical inclusion with a three-axis dilatation were derived in Ref. [67] using the equations of mechanical equilibrium. In Ref. [68] the elastic displacements, strains and stresses of a spherical inclusion with a one-axis dilatation were obtained through a continuous distribution of circular dislocation loops over the sphere surface. Recently, the stress fields of the inclusions having the shape of a semi-sphere [69] and finite-height cylinder [70] have been calculated using the Green function method.

In the above solutions [61-68] for ellipsoidal inclusions their elastic strains and stresses had no singularities. It is not the case, however, for facetted inclusions. The first solution by Goodier [60] for a rectangular inclusion in a thin plate already demonstrated that in the vertices of the rectangular boundary, the shear strains and stresses were singular. An extension of Goodier's solution to the case of a heated parallelepipedic inclusion was done by Ignachek and Nowacki in 1958 and published in book [71]. The thermal stresses created by a finite number of parallelepipedic inclusions were calculated in Ref. [72], whose results were also published in book [73]. The elastic fields of isotropic parallelepipedic inclusions with an arbitrary eigenstrain were derived in Refs. [74-77]. In particular, Faivre has shown [75] that if the inclusion eigenstrain is a pure dilatation, then the elastic dilatation is uniform inside the inclusion and equal to zero outside it. As a result, the strain energy of such an inclusion does not depend on its shape.

Last years a few problems for isotropic inclusions with a shape of polygons and polyhedrons have also been solved [25,29,78-84]. In particular, using the Green function approach, Pearson and Faux have obtained the stress field of a truncated pyramidal inclusion in an isotropic infinite medium [29]. Faux *et al.* have calculated the strain field of a wire inclusion with an arbitrary cross section [25]. Gosling and Willis have calculated the elastic fields of wire inclusions with a trapezoidal cross section [78]. Although in general, elastic strains inside polygonal and polyhedral inclusions are not uniform [79,81], Mura has shown [82,83] that there are inclusions having the shape of polygons of special kind, which create inside themselves a uniform strain field. Thus, it has appeared that the ellipsoidal inclusions are not the only kind of inclusions, which create uniform elastic strains in their internal regions.

Most of the solutions for isotropic inclusions in an infinite medium have also been extended to the case of inclusions in a half-space. Apparently, the first problem about an inclusion in a semi-infinite medium was solved by Mindlin and Cheng [85] for a spherical inclusion with a uniform eigenstrain induced by the difference in the thermal expansion coefficients of the inclusion and the matrix. More recently, this solution has been generalized to the case of an arbitrary eigenstrain [86]. Seo and Mura have obtained the solution for an ellipsoidal inclusion with a dilatational eigenstrain [87]. Yu and Sanday have solved the problem about an axisymmetric inclusion with a dilatation and a uniform tensile strain [88]. The interaction of a spherical inclusion with a free surface has been examined by Maradulin and Wallis [89] and Loges *et al.* [90]. Maradulin and Wallis [89] have also analyzed the interaction of dilatation centers near a flat free surface. Finally, the solution for a semispherical inclusion in a half-space has recently been obtained by Wu [91].

Apparently, the first calculation of the elastic fields of a facetted inclusion in a half-space was performed by Chiu [92]. Chiu considered a parallelepipedic inclusion lying in such a way that one of its facets was parallel to a free surface. The inclusion was supposed to have an arbitrary dilatational eigenstrain, and the solution for its elastic fields was obtained in terms of the Legendre polynomials. More recently, Hu obtained an alternative solution [93] for the stress field of a dilatational parallelepipedic inclusion outside this inclusion. The solutions of Chiu [92] and Hu [93] were extended by Glas [94], who calculated not only the elastic stresses and strains but also the displacements of a dilatational parallelepipedic inclusion in a half-space, as well as the strain energy of such an inclusion. In contrast to the solution of Hu [93], the explicit solution given by Glas [94] describes the elastic fields both outside and inside the inclusion. The solution of Hu [93] was obtained by integrating the elastic fields created by point sources of expansion over the in-

clusion volume. The solution of Glas [94] for a parallelepipedic inclusion was obtained using the expressions (also derived in Ref. [94]) for the elastic displacements of a platelike dilatational inclusion whose eigenstrain varied in one direction in an oscillatory manner. Such a platelike inclusion may model, in particular, a film with an alternating chemical composition, embedded into a matrix. As a limiting case of the parallelepipedic inclusion, Hu [93] and Glas [94] also calculated the elastic fields of a wire inclusion with a rectangular cross section, parallel to a free surface. The expressions for the stress field created in a half-space by an infinite wire inclusion with a rectangular cross section were also obtained by Gutkin in 1987 using the solution [95] for the stress field of such an inclusion in a finite-thickness plate. These expressions are given in Ref. [96]. Finally, the displacement field created by an array of infinite rectangular wire inclusions in a half-space was derived by Kaganer *et al.* [47].

Using the expressions [94] for the displacements created by a parallelepipedic inclusion in a half-space, Glas [35,36] calculated the elastic fields of the inclusions with the shapes of a truncated pyramid and infinite trapezoidal wire. (A partial case of the first of these problem has been considered in Ref. [43] where the average normal stress and dilatation created by a subsurface pyramidal inclusion at a flat free surface were calculated). More recently, Glas [37] used the solution for a single trapezoidal wire inclusion for the calculation of the elastic fields of an array of such inclusions and generalized this solution to the case of arbitrary facetted wire inclusions of infinite length. As a limiting case of the solution for the trapezoidal wire inclusions in a half-space, Glas derived the explicit expressions for the elastic fields of such inclusion in an infinite medium [37]. For the calculation of the elastic fields of pyramidal and wire inclusions in a half-space, the latter were modeled by continuous distributions of infinitely thin parallelepipedic inclusions [35,36]. The same approach was used for the calculation of the displacements and strains induced by a finite-length circular cylindrical inclusion parallel to a flat free surface [41]. As a limiting case of solution [41], Glas obtained the elastic fields induced by a semi-infinite and infinite cylindrical inclusion in a half-space and by a finite-length cylindrical inclusion in an infinite solid. Solution [41] for a cylinder of finite length, parallel to a free surface, amplified the previous solutions for the finite-length cylinder perpendicular to a flat free surface [97-99].

The solutions of many problems on inclusions in an infinite or semi-infinite medium are also extended to the case of a two-phase infinite medium with a flat interphase boundary. In these problems, both phases are supposed to be elastically isotropic but have different elastic moduli. When considering two-phase mediums, one distinguishes two kinds of interphase boundaries: coherent and gliding ones. For both kinds of interphase boundaries, all the displacements and the stresses normal to the boundary must be continuous at the interface. Besides, at the coherent boundary, the stress components tangential to the boundary must be continuous, whereas at the gliding interface these stress components have to vanish. Most of the problems on inclusions in two-phase mediums are solved for coherent interfaces, although there are also solutions for gliding interfaces. The simplest problems about inclusions in a two-phase medium include the problems about a dilatation center [100,101], spherical inclusion with an arbitrary homogeneous eigenstrain [102], and deformation center [103]. Following Mindlin [104], Yu and Sanday [103] define the deformation center as a unit point force, a dipole of such forces, or a dilatation center. On the basis of the solution for a deformation center, Yu and Sanday derived a general solution for a uniform inclusion of arbitrary shape near a flat interface [105]. The solution was obtained for both a coherent and a gliding interface. In the limiting case where the elastic moduli of one of the phases were set to equal zero and the inclusion shape was assumed to be ellipdoidal or axisymmetrical, Yu and Sanday obtained the known results [88,90] for inclusions at a free surface.

Yu and Sanday obtained the general solution [105] for an arbitrary inclusion in a two-phase medium by integration of the elastic fields, created in such a medium by a deformation center, over the inclusion volume. Shortly before Yu and Sanday, Hu applied a similar technique for the calculation of the stresses induced by a parallelepipedic inclusion in a half-space [93]. Note that, similar to the case of an infinite medium, the elastic fields of an arbitrary inclusion in a half-space or two-phase medium may be obtained using the Green function method, that is, through integration of the elastic fields created by a unit point force over the inclusion volume. The Green function method was used in Ref. [106] for the calculation of the elastic fields and strain energy of a cylindrical and a spherical inclusion as well as for the solution of the problem about an arbitrary axisymmetric inclusion near an

interface [107]. Along with the problems on inclusions in a two-phase 3D medium, the solutions of 2D problems for arbitrary inclusions in a two-phase plane were also derived [108,109]. These problems were solved using the conformal mapping approach.

Besides the problems on inclusions in a one- or two-phase infinite medium or half-space, several authors solved the problems about inclusions in a finite-thickness plate and infinite cylinder. For example, Malyshev *et al.* [95] calculated the stress field of an infinite wire with a rectangular cross section, whose axis is parallel to the plate surfaces. The solution of this problem was obtained on the basis of the expressions for the stress field of such an inclusion in an infinite medium using the virtual surface dislocation method [110]. In this approach, the stress field of the inclusion in a plate was presented as the sum of the stress field of such an inclusion in an infinite medium and the stress fields of virtual dislocations continuously distributed over the plate free surfaces. The dislocation distribution densities were found from the boundary conditions at the plate free surfaces by solving appropriate integral equations.

Another problem for an inclusion in a finite-thickness plate is the problem about a dilatation center. The solution of this problem was given by Yu and Sanday [111] and amplifies the previous solution of these authors for a deformation center in a two-phase medium [103]. Using the solution for the dilatation center, Yu and Sanday obtained the general solution for an arbitrary dilatational inclusion in a plate [111]. As an illustration of the general solution obtained, they also examined a spherical inclusion in a plate [111]. More recently, Chang *et al.* [112] solved the problem about another kind of inclusion in a plate, namely about cylindrical inclusion perpendicular to the plate surfaces. This solution supplements with the solutions for such a cylindrical inclusion in a half-space [97-99]. Besides the solutions for inclusions in a plate, note the solution for an infinite cylindrical inclusion with a uniform dilatational eigenstrain, lying in a cylindrical matrix and coaxial to this matrix [113].

Many solutions for inclusions in isotropic solids were also generalized to the case of elastic anisotropy. In particular, the elastic fields of cylindrical inclusions in anisotropic infinite solids were obtained in Refs. [114,115] using the complex potential method. Willis extended solution [114] to the case of cubic symmetry [116]. The subsequent analysis was also performed for elliptic inclusions in an orthotropic medium [117,118] and a medium with one symmetry plane [119]. The problem on an ellipsoidal inclusion in an infinite anisotropic medium was examined by Asaro and Barnett [120], Mura [59], and Kunin and Sosnina [121]. Andreev *et al.* obtained in an integral form the strain field created in an infinite cubic crystal by a spherical, cubic, pyramidal, semispherical, truncated pyramidal and finite-length cylindrical inclusion [27]. Holy *et al.* considered the problem about a dilatation center in an anisotropic semi-infinite cubic crystal [28]. Yang and Chou derived the solutions for the generalized plane [122] and antiplane [123] 2D problems about elliptical inclusions in an infinite anisotropic medium. More recently, solution [123] of the antiplane problem for an elliptical inclusion in an anisotropic infinite medium was extended to the case of an anisotropic half-space [124] and two-phase anisotropic medium [125]. Recently, Ru obtained a general solution for an inclusion of arbitrary shape in an anisotropic plane or half-plane [126].

Thus, at present, there are a large number of analytical solutions for the elastic fields of inclusions of different shapes in isotropic and anisotropic infinite and semi-infinite mediums, cylinders and plates. Apparently, the most powerful tool for deriving the elastic fields of inclusions in infinite and semi-infinite solids is the Green function method. Since this method is widely used for the calculation of the elastic fields of nanocomposites, we will describe it in the next section.

3. GREEN FUNCTION METHOD

Following Kröner [127], present the total strain $\in_{ij}$ acting in a solid as the sum of the elastic strain ε_{ij} and inelastic strain (eigenstrain) $\widetilde{\varepsilon}^{*}_{ij}$: $\in_{ij} = \varepsilon_{ij} + \widetilde{\varepsilon}^{*}_{ij}$. If the solid contains an inclusion that occupies a 3D domain Ω, the eigenstrain $\widetilde{\varepsilon}^{*}_{ij}$ may be presented as $\widetilde{\varepsilon}^{*}_{ij} = \varepsilon^{*}_{ij} g(\boldsymbol{x})$, where $\boldsymbol{x} = (x_1, x_2, x_3)$ is a point in a coordinate space, $g(\boldsymbol{x})=1$ if the point $\boldsymbol{x}$ lies inside the region Ω, and $g(\boldsymbol{x})=0$ otherwise. The relation $\widetilde{\varepsilon}^{*}_{ij} = \varepsilon^{*}_{ij} g(\boldsymbol{x})$ means that the eigenstrain is equal to ε^{*}_{ij} inside the inclusion and to zero outside the inclusion.

The Green function method allows one to calculate the elastic fields of an inclusion using as an input the inclusion eigenstrain ε^{*}_{ij} and its size and shape (which are charaterized by the function $g(\boldsymbol{x})$). According to [59], the displacements u_i, created by an inclusion in a composite solid, are given by

$$u_i(x) = \int_V C_{jlmn} \widetilde{\varepsilon}^{*}_{mn}(\boldsymbol{x}') \frac{\partial}{\partial \boldsymbol{x}'_l} G_{ij}(\boldsymbol{x}, \boldsymbol{x}') d\boldsymbol{x}'. \qquad (1)$$

In formula (1) $\boldsymbol{x}'=(x_1', x_2', x_3')$ is a 3D vector, $d\boldsymbol{x}'=dx_1'dx_2'dx_3'$, V is the region occupied by the composite solid in the coordinate space (x_1', x_2', x_3'), C_{jlmn} is the tensor of elastic moduli, and $G_{ij}(\boldsymbol{x}, \boldsymbol{x}')$ is the elastostatic Green tensor of a medium. If the inclusion eigenstrain is uniform (that is, ε^*_{mn} = const), formula (1) may be written as

$$u_i(\boldsymbol{x}) = C_{jlmn}\varepsilon^*_{mn}\int_{\Omega}\frac{\partial}{\partial x_l'}G_{ij}(\boldsymbol{x},\boldsymbol{x}')d\boldsymbol{x}' \qquad (2)$$

or presented through an integral over the inclusion boundary $|\Omega|$ [59]:

$$u_i(\boldsymbol{x}) = C_{jlmn}\varepsilon^*_{mn}\int_{|\Omega|}G_{ij}(\boldsymbol{x},\boldsymbol{x}')n_l(\boldsymbol{x}')dS(\boldsymbol{x}'). \qquad (3)$$

In formula (3) $\boldsymbol{n}$ denotes the external normal to the surface $|\Omega|$.

The values of the Green functions G_{ij}, appearing in formulae (1)–(3), are numerically equal to the displacements $\tilde{u}_i$, created at the point $\boldsymbol{x}$ by a unit point force acting at the point $\boldsymbol{x}'$ in the direction of the x_j-axis. In the case of an infinite medium, the Green tensor depends on the difference $\boldsymbol{x}$-$\boldsymbol{x}'$ only. The expressions for the Green functions for an infinite isotropic medium were originally derived by Kelvin [128] and have the following form [59]:

$$G_{kl}(\boldsymbol{x}-\boldsymbol{x}') = \frac{1}{16\pi\mu(1-\nu)R}\left\{(3-4\nu)\delta_{kl}+\frac{(x_k-x_k')(x_l-x_l')}{R^2}\right\}, \qquad (4)$$

where $R=[(x_1-x_1')^2+(x_2-x_2')^2+(x_3-x_3')^2]^{1/2}$, δ_{kl} is the Kronecker delta, equal to 1 if $k=l$ and to 0 if $k \neq l$, μ is the shear modulus, and ν is the Poisson ratio. The Green functions for different infinite anisotropic mediums were also obtained in different forms [129-143].

The Green tensor for a semi-infinite isotropic medium $x_3 \geq 0$ was obtained by Mindlin [104]. Notice that the expressions for the Green functions given in Ref. [104] contain a sign error, which was corrected by Mindlin in 1975 in a private communication. In the corrected form, the expressions for the Green functions of a semi-infinite isotropic medium $x_3 \geq 0$ are given in Mura's book [59] and have the following form (in units of $1/[16\pi\mu(1-\nu)]$):

$$G_{ij}(\boldsymbol{x},\boldsymbol{x}') = G_{ji}(\boldsymbol{x},\boldsymbol{x}') = \left\{\frac{3-4\nu}{R_1}+\frac{4(1-\nu)(1-2\nu)}{R_2+x_3+x_3'}+\frac{R_2^2+2x_3x_3'}{R_2^3}\right\}\delta_{ij} + (x_i-x_i')(x_j-x_j')\times\left\{\frac{1}{R_1^3}+\frac{4(1-\nu)(1-2\nu)}{R_2(R_2+x_3+x_3')^2}+\frac{(3-4\nu)R_2^2-6x_3x_3'}{R_2^5}\right\}, \qquad (5a)$$

$$G_{3j}(\boldsymbol{x},\boldsymbol{x}') = (x_j-x_j')\left\{(x_3-x_3')\left[\frac{1}{R_1^3}+\frac{3-4\nu}{R_2^3}\right]+\frac{4(1-\nu)(1-2\nu)}{R_2(R_2+x_3+x_3')}-\frac{6x_3x_3'(x_3+x_3')}{R_2^5}\right\}, \qquad (5b)$$

$$G_{i3}(\boldsymbol{x},\boldsymbol{x}') = (x_i-x_i')\left\{(x_3-x_3')\left[\frac{1}{R_1^3}+\frac{3-4\nu}{R_2^3}\right]-\frac{4(1-\nu)(1-2\nu)}{R_2(R_2+x_3+x_3')}+\frac{6x_3x_3'(x_3+x_3')}{R_2^5}\right\}, \qquad (5c)$$

$$G_{33}(\boldsymbol{x},\boldsymbol{x}') = \frac{3-4\nu}{R_1}+\frac{(x_3-x_3')^2}{R_1^3}+\frac{8(1-\nu)^2-(3-4\nu)}{R_2}+\frac{(3-4\nu)(x_3+x_3')^2-2x_3x_3'}{R_2^3}+\frac{6x_3x_3'(x_3+x_3')^2}{R_2^5}, \qquad (5d)$$

where $i,j=1,2$ and $R_{1,2}=(x_1-x_1')^2+(x_2-x_2')^2+(x_3\pm x_3')^2$.

It should be noted that the Green functions given by formulae (5) provide the displacements created by a unit point force inside a semi-infinite solid. The problem of finding the displacements induced by such a force in a semi-infinite solid is called the Mindlin problem. Another problem refers to the situations where a point force is applied at the surface of a semi-infinite solid from outside. This problem is called the Boussinesq problem. For both classes of problems, the functions relating the applied force and the displacements induced by it are referred to as Green functions. However, here we will not discuss the Green functions arising in the Boussinesq problem and restrict ourselves to the Green functions for the Mindlin problem. For a detailed consideration of the Boussinesq problem for anisotropic solids, the reader is referred to recent review [144].

The Green functions for anisotropic semi-infinite solids have been obtained in an integral form by Portz and Maradulin [145] for the case of cubic crystals. Later, the Green functions for anisotropic half-spaces have been derived by Walker [146] and by Pan [147].

For the isotropic case, the Green tensors are also obtained for a two-phase medium with a coherent interface [148] and gliding interface [149]. The expressions for the Green tensors of such mediums are also given in book [59].

After the calculation of the inclusion displacements u_i using formula (1), it is easy to derive the expressions for the inclusion total strains $\in_{ij}$ and stresses σ_{ij}. The total strains $\in_{ij}$ are written in terms of the displacements u_i as

$$\in_{ij} = \frac{1}{2}(u_{i,j} + u_{j,i}). \tag{6}$$

With the aid of Hooke's law and the relation $\varepsilon_{kl} = \in_{kl} - \tilde{\varepsilon}^*_{kl}$, the stresses σ_{ij} are presented in terms of the strains $\in_{ij}$ as

$$\sigma_{ij} = C_{ijkl}\varepsilon_{kl} = C_{ijkl}(\in_{kl} - \tilde{\varepsilon}^*_{kl}). \tag{7}$$

In the mediums where exact closed-form analytical expressions for the Green functions exist, the inclusion displacements, strains and stresses may be directly calculated using formulae (1), (6), and (7). However, for most of anisotropic solids, the Green functions may be obtained only in the form of integrals or series. Therefore, in many cases, especially for anisotropic solids, it is more convenient to use the expressions for the Fourier images of the Green functions.

For an infinite medium, the Green functions depend on the coordinate difference $\boldsymbol{x}$-$\boldsymbol{x}$' only. This allows one to apply the convolution theorem to the right-hand side of formula (1). Using this theorem, 3D Fourier images $\hat{u}_p$ and $\hat{\in}_{pq}$ of the inclusion displacements and strains are written in terms of 3D Fourier images $\hat{G}_{pq}$ of the Green functions $G_{pq}(\boldsymbol{x}\text{-}\boldsymbol{x}')$. (Here and in the following the 3D Fourier transforms of arbitrary functions $f(\boldsymbol{x})$ are defined by the relation $\hat{f}(\boldsymbol{k}) = \int_{-\infty}^{+\infty}\int\int\int f(\boldsymbol{x})\exp(\mathrm{i}\boldsymbol{k}\cdot x)d\boldsymbol{x}$, where $\mathrm{i} = \sqrt{-1}$). For this purpose, we modify formula (1), replacing in this formula $G_{ij}(\boldsymbol{x}, \boldsymbol{x}')$ by $G_{ij}(\boldsymbol{x}\text{-}\boldsymbol{x}')$ and put V to be an unbounded 3D region. Applying the convolution theorem to the resulting equation and accounting for the relation $\tilde{\varepsilon}^*_{mn} = \varepsilon^*_{mn} g(\boldsymbol{x})$, formula (6) and equality $\varepsilon_{pq} = \in_{pq} - \varepsilon^*_{pq} g(\boldsymbol{x})$, one obtains:

$$\hat{u}_p(\boldsymbol{k}) = -\mathrm{i}\boldsymbol{k}_l C_{jlmn}\varepsilon^*_{mn}\hat{g}\hat{G}_{pj}, \tag{8a}$$

$$\hat{\varepsilon}_{pq}(\boldsymbol{k}) = -\frac{\mathrm{i}}{2}(\boldsymbol{k}_q\hat{u}_p + \boldsymbol{k}_p\hat{u}_q) - \varepsilon^*_{pq}\hat{g}. \tag{8b}$$

From the definition of the function $g(\boldsymbol{x})$ (equal to 1 inside the region Ω and to 0 outside it) it follows that the expression for the Fourier image $\hat{g}(\boldsymbol{k})$ of this function has the following form: $\hat{g}(\boldsymbol{k}) = \int_\Omega \exp(\mathrm{i}\,\boldsymbol{k}\cdot\boldsymbol{x})d\boldsymbol{x}$. Now the displacements u_p and elastic strains ε_{pq} are cast using the reverse Fourier transform as

$$u_p(\boldsymbol{x}) = \frac{1}{(2\pi)^3}\int_{V_k}\hat{u}_p(\boldsymbol{k})\exp(\mathrm{i}\,\boldsymbol{k}\cdot\boldsymbol{x})dV_k',$$

$$u_p(\boldsymbol{x}) = \frac{1}{(2\pi)^3}\int_{V_k}\hat{\varepsilon}_{pq}(\boldsymbol{k})\exp(\mathrm{i}\,\boldsymbol{k}\cdot\boldsymbol{x})dV_k', \tag{9}$$

In formula (9) dV_k' is the volume element of the Fourier space, and integration is performed over the whole infinite volume V_k of this space.

For an isotropic infinite medium, we have [59]:

$$C_{jlmn} = \lambda\delta_{jl}\delta_{mn} + \mu(\delta_{jm}\delta_{ln} + \delta_{jn}\delta_{lm}), \tag{10}$$

$$\hat{G}_{ij} = \frac{(\lambda + 2\mu)k^2\delta_{ij} - (\lambda + \mu)k_i k_j}{\mu(\lambda + 2\mu)k^4}, \tag{11}$$

where $\lambda = 2\nu\mu/(1\text{-}2\nu)$ and $k^2 = \boldsymbol{k}\cdot\boldsymbol{k}$.

For an infinite cubic crystal characterized by 3 elastic moduli, c_{11}, c_{12} and c_{44}, the tensor of elastic moduli and the Green tensor follow as [27,59]

$$C_{ijkl} = c_{12}\delta_{ij}\delta_{kl} + c_{44}(\delta_{ik}\delta_{jl} + \delta_{il}\delta_{jk}) + c_{an}\delta_{ijkl}, \tag{12}$$

$$\hat{G}_{ij} = \frac{\delta_{ij}}{c_{44}k^2 + c_{an}k_i^2} - \frac{(c_{12} + c_{44})k_i k_j}{(c_{44}k^2 + c_{an}k_i^2)(c_{44}k^2 + c_{an}k_j^2)} \times \left\{1 + (c_{12} + c_{44})\sum_{p=1}^{3}\frac{k_p^2}{c_{44}k^2 + c_{an}k_p^2}\right\}^{-1}, \tag{13}$$

where $\delta_{ijkl}=1$ for $i=j=k=l$ and $\delta_{ijkl}=0$ otherwise, and $c_{an}=c_{11}\text{-}c_{12}\text{-}2c_{44}$.

Thus, for a specified medium characterized by the tensor $\hat{G}_{pq}$, the displacements and elastic strains induced by inclusions of different sizes and shapes are calculated in the same manner using formulae (8) and (9). In these formulae, the size and shape of

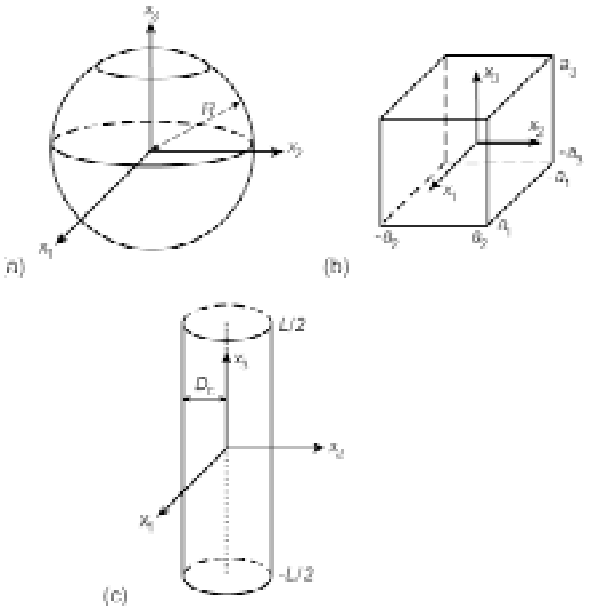

Fig.1. Geometry of model inclusions in a cubic crystal. (a) Spherical inclusion. (b) Cubic inclusion. (c) Finite-length cylindrical inclusion.

the inclusion that occupies the region Ω are accounted for in the expression for the function $\hat{g}(\boldsymbol{k})$ only.

Recently, Andreev *et al.* have calculated the elastic strains created by the inclusions of different shapes in infinite isotropic and cubic crystals [27]. For the calculation of strains induced by inclusions in cubic crystals, they also calculated the functions $\hat{g}(\boldsymbol{k})$ for the case of a cubic crystal and different inclusion shapes: sphere, cube, pyramid, truncated pyramid, semisphere and finite-length cylinder. For the inclusions with high symmetry these functions have a simple form. For example, for a spherical inclusion of radius R, whose center lies at the origin of the coordinate system (x_1, x_2, x_3) (Fig. 1a),

$$\hat{g}(\boldsymbol{k}) = \frac{4\pi(\sin kR - kR\cos kR)}{k^3}. \qquad (14)$$

For a cubic inclusion with the center at the origin of the coordinate system, faces parallel to the coordinate axes x_1, x_2, and x_3, and the lengths of the corresponding sides a_1, a_2, and a_3 (Fig. 1b),

$$\hat{g}(\boldsymbol{k}) = \frac{8}{k_1 k_2 k_3}\sin\left(\frac{k_1 a_1}{2}\right)\sin\left(\frac{k_2 a_2}{2}\right)\sin\left(\frac{k_3 a_3}{2}\right). \qquad (15)$$

For a cylindrical inclusion of length L and diameter D_c, with the center at the origin of the coordinate system whose x_3-axis coincides with the cylinder axis (Fig. 1c),

$$\hat{g}(\boldsymbol{k}) = \frac{2\pi D_c}{k_{\|}k_3}\sin(k_3 L/2)J_1(D_c k_{\|}/2), \qquad (16)$$

where $k_{\|}=(k_1^2+k_2^2)^{1/2}$ and $J_1(t)$ is the Bessel function of the first kind of the first order.

The simple inclusion shapes analyzed by Andreev *et al.* [27] are convenient to study the effect of elastic anisotropy on inclusion elastic fields. Andreev *et al.* [27] have shown that in the case of composite solids with cubic symmetry elastic anisotropy essentially influences the strains created by a spherical inclusion but does not seriously affect the strains created by a cubic or a pyramidal inclusion. Thus, the effect of elastic anisotropy on the inclusion elastic fields is essential for an inclusion with an isotropic shape. However, as the inclusion shape becomes more anisotropic, the effect of elastic anisotropy on the inclusion elastic fields diminishes.

In some cases, the use of the Fourier images of the Green functions is convenient for the calculation of the inclusion displacements, strains and stresses not only in infinite, but also in semi-infinite composite solids. For a semi-infinite solid occupying the region $x_3 \geq 0$ the Green functions depend on the coordinates x_3 and x_3' as well as on the coordinate differences x_1-x_1' and x_2-x_2'. In other words, in the situation discussed, the Green functions $G_{pq}(\boldsymbol{x},\boldsymbol{x}')$ may be presented as $G_{pq}(\boldsymbol{x},\boldsymbol{x}') = \tilde{G}_{pq}(x_1 - x_1', x_2 - x_2', x_3, x_3')$. Consequently, instead of the 3D Fourier transform employed for the calculation of the inclusion elastic fields in an infinite medium, the inclusion elastic fields in a half-space may be calculated using the 2D Fourier transform in the coordinate space (x_1, x_2). The procedure of calculation of the inclusion elastic fields in a half-space, exploiting the 2D Fourier transform, is similar to the calculation technique applied in the case of an infinite medium. This calculation procedure works in the cases where the expressions for 2D Fourier images, $\hat{G}_{pq}^{2D}(k_1, k_2, x_3, x_3') = \int_{-\infty}^{+\infty}\int \tilde{G}_{pq}(\bar{x}_1, \bar{x}_2, x_3, x_3')\exp[-\mathrm{i}(k_1\bar{x}_1 + k_2\bar{x}_2)]d\bar{x}_1 d\bar{x}_2$, of the Green functions are available. The exact analytical expressions for the 2D Fourier images of the Green functions are obtained, for example, for a semi-infinite cubic crystal [145]. These expressions have been applied in the calculation of the elastic interaction of quantum dots (nanoscopic semiconductor inclusions) in semiconductor nanocomposites [8,150].

4. INTEGRATION OF EQUATIONS OF EQUILIBRIUM

In some simple problems about inclusions, their elastic fields may be derived through a direct solution of the equations of the elasticity theory written in terms of displacements. These equations are obtained by the substitution of Hooke's law and strain-displacements relations to the equations of mechanical equilibrium. Such an approach was used, in particular, for solving the problem about the thermal stresses arising after the contact of two solids with different thermal expansion coefficient [59,151] and for the calculation of the stresses created by an infinite cylindrical nanoinclusion with a dilatational eigenstrain in an infinite nanocomposite [67]. In the present section, we illustrate this approach with an example of the problem about misfit stresses in an infinite two-phase composite nanowire.

Consider a two-phase nanowire of radius R, which consists of a cylindrical substrate (inclusion) of radius R_0 and a film of thickness H (H=R-R_0) (Fig. 2). The film and substrate are assumed to be isotropic solids with equal shear moduli μ and Poisson ratios ν but different crystal lattice parameters. The dilatational misfit of the parameters, a_f and a_s, of the film and substrate crystal lattices is characterized by the parameter f=2(a_f-a_s)/(a_f+a_s) and creates elastic strains and stresses in the composite nanowire.

Let $\varepsilon_{ij}^{*(k)}$ be the tensor of misfit strain in the k-th region, where k=1 for the wire substrate and k=2 for the film (Fig. 2). Let us suppose that $\varepsilon_{ij}^{*(2)}$=0. In the simple case of a dilatational misfit we assume $\varepsilon_{ij}^{*(2)}$=$f\delta_{ij}$. The total strain $\in_{ij}^{(k)}$ in the wire composite is the sum of the misfit strain $\varepsilon_{ij}^{*(k)}$ and elastic strain $\varepsilon_{ij}^{(k)}$:

$$\in_{ij}^{(k)} = \varepsilon_{ij}^{*(k)} + \varepsilon_{ij}^{(k)}. \tag{17}$$

In the cylindrical coordinate system whose z-axis coincides with the cylinder axis, the total strain tensor components are expressed via displacement as follows [151]:

$$\in_{rr}^{(k)} = \frac{\partial u_r^{(k)}}{\partial r}, \quad \in_{\theta\theta}^{(k)} = \frac{u_r^{(k)}}{r}, \quad \in_{zz}^{(k)} = \frac{\partial u_z^{(k)}}{\partial z} = 0. \tag{18}$$

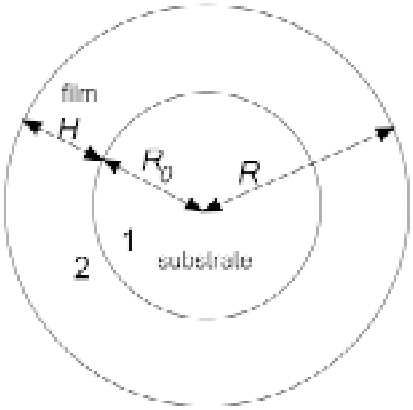

Fig. 2. Two-phase misfitting nanowire.

The stress tensor can be written using Hooke's law [151] as

$$\sigma_{ij}^{(k)} = 2\mu\left(\varepsilon_{ij}^{(k)} + \frac{v}{1-2v}\varepsilon^{(k)}\right), \tag{19}$$

where $\varepsilon^{(k)}$=$\varepsilon_{ii}^{(k)}$. In the cylindrical coordinate system the components of the stress tensor are as follows:

$$\sigma_{rr}^{(1)} = 2\mu\left(\in_{rr}^{(1)} + \frac{v}{1-2v}\in^{(1)} - \frac{1+v}{1-2v}f\right), \tag{20a}$$

$$\sigma_{\theta\theta}^{(1)} = 2\mu\left(\in_{\theta\theta}^{(1)} + \frac{v}{1-2v}\in^{(1)} - \frac{1+v}{1-2v}f\right), \tag{20b}$$

$$\sigma_{zz}^{(1)} = 2\mu\,\frac{v\in^{(1)} -(1+v)f}{1-2v}, \tag{20c}$$

$$\sigma_{ij}^{(2)} = 2\mu\left(\in_{ij}^{(2)} + \frac{v}{1-2v}\in^{(2)}\right), \tag{20d}$$

where $\in^{(k)}$= $\in_{ii}^{(k)}$. From the equation of mechanical equilibrium [151]

$$\frac{\partial\sigma_{rr}}{\partial r} + \frac{\sigma_{rr}-\sigma_{\theta\theta}}{r} = 0 \tag{21}$$

and formulae (18) and (20) we obtain the following differential equation for displacements:

$$\frac{d^2u_r^{(k)}}{dr^2} + \frac{1}{r}\frac{du_r^{(k)}}{dr} - \frac{u_r^{(k)}}{r^2} = 0. \tag{22}$$

The solution of this equation is

$$u_r^{(k)} = A_k r + \frac{B_k}{r}, \tag{23}$$

where the constants A_k and B_k are derived from the boundary conditions

$$\begin{aligned} &u_r^{(1)}(r \to 0) \text{ is limited,} \\ &u_r^{(1)}(r = R_0) = u_r^{(2)}(r = R_0), \\ &\sigma_{rr}^{(1)}(r = R_0) = \sigma_{rr}^{(2)}(r = R_0), \\ &\sigma_{rr}^{(2)}(r = R) = 0. \end{aligned} \tag{24}$$

The solution of system (24) yields

$$\begin{aligned} &A_1 = \frac{1+v}{1-v}\frac{f}{2}\frac{R^2 + (1-2v)R_0^2}{R^2}, \quad B_1 = 0, \\ &A_2 = A_1 - \frac{1+v}{1-v}\frac{f}{2}, \quad B_2 = \frac{1+v}{1-v}\frac{f}{2}R_0^2. \end{aligned} \tag{25}$$

The stresses σ_{ij}^f in the two-phase nanowire, hereafter referred to as misfit stresses (equal to $\sigma_{ij}^{(1)}$ at $r<R_0$, and to $\sigma_{ij}^{(2)}$ at $r>R_0$), follow from formulae (18), (20), (23) and (25) as

$$\sigma_{rr}^f = \sigma^*\left(\frac{R_0^2 - R^2}{R^2}\Theta(R_0 - r) + \frac{R_0^2}{R^2}\frac{r^2 - R^2}{r^2}\Theta(r - R_0)\right), \tag{26a}$$

$$\sigma_{\theta\theta}^f = \sigma^*\left(\frac{R_0^2 - R^2}{R^2}\Theta(R_0 - r) + \frac{R_0^2}{R^2}\frac{r^2 + R^2}{r^2}\Theta(r - R_0)\right), \tag{26b}$$

$$\sigma_{zz}^f = 2\sigma^*\left(\frac{vR_0^2 - R^2}{R^2}\Theta(R_0 - r) + \frac{vR_0^2}{R^2}\Theta(r - R_0)\right), \tag{26c}$$

where $\sigma^*=\mu f(1+\nu)/(1-\nu)$ and $\Theta(x)$ is the Heavyside function ($\Theta(x)=1$ for $x>0$, and $\Theta(x)=0$ for $x<0$).

The above expressions for the misfit stresses in a composite nanowire have been used for the calculation of the conditions for the formation of different misfit defects in such a nanowire [113,152,153].

5. METHOD OF SURFACE DISLOCATION LOOPS

In the previous sections we have considered the methods for the calculation of the elastic fields of inclusions, based on the use of the Green tensor or direct integration of the equations of equilibrium. Another approach alternative to these methods rests on the concept of virtual surface dislocations. In a general form, this approach has first been formulated by Kroupa and Lejček [110]. It is based on the continuous distribution of virtual dislocations and/or dislocation loops over the inclusion boundary. If the total tensor of eigenstrains induced by such defects equals to the inclusion eigenstrain tensor, then the inclusion displacements, strains and stresses are equal to the total displacements, strains and stresses, respectively, created by virtual surface dislocations and/or dislocation loops.

Examples of the distributions of surface dislocations and dislocation loops that model inclusions with dilatational eigenstrains are given in Fig. 3. Fig. 3a illustrates the film inclusion on a substrate, which is characterized by the only nonvanishing component $\varepsilon_{xx}^* = \varepsilon^*$ of the eigenstrain tensor. The eigenstrain of such an inclusion is modeled by an array of edge dislocations continuously distributed over the film-substrate interface with the linear density ε^*/b, where b is the dislocation Burgers vector magnitude. In Fig. 3b the spherical inclusion with a one-axis eigenstrain ε_{zz}^* is modeled by a continuous distribution of circular prismatic dislocation loops over the sphere surface [68]. Lastly, in Fig. 3c the parallelepipedic inclusion with a three-axis dilatational eigenstrain $\varepsilon_{ij}^*=\varepsilon^*\delta_{ij}$ is modeled by three orthogonal ensembles of rectangular prismatic dislocation loops distributed with the linear density ε^*/b [154]. In the case where such an inclusion lies in an infinite isotropic solid, the inclusion stress field (equal to the total stress field of the virtual dislocation loops distributed over the inclusion surface) is given by [154]:

$$\sigma_{ij}(x,y,z) = C\Phi_{ij}(x - x', y - y', z - z')\Big|_{x' = x_1}^{x' = x_2}\Big|_{y' = y_1}^{y' = y_2}\Big|_{z' = z_1}^{z' = z_2}, \tag{27}$$

where

$$\begin{aligned} \Phi_{xx} &= \arctan\frac{\bar{x}R_1}{\bar{y}\,\bar{z}}, \\ \Phi_{yy} &= \arctan\frac{\bar{y}R_1}{\bar{x}\,\bar{z}}, \\ \Phi_{zz} &= \arctan\frac{\bar{z}R_1}{\bar{x}\,\bar{y}}, \end{aligned} \tag{28}$$

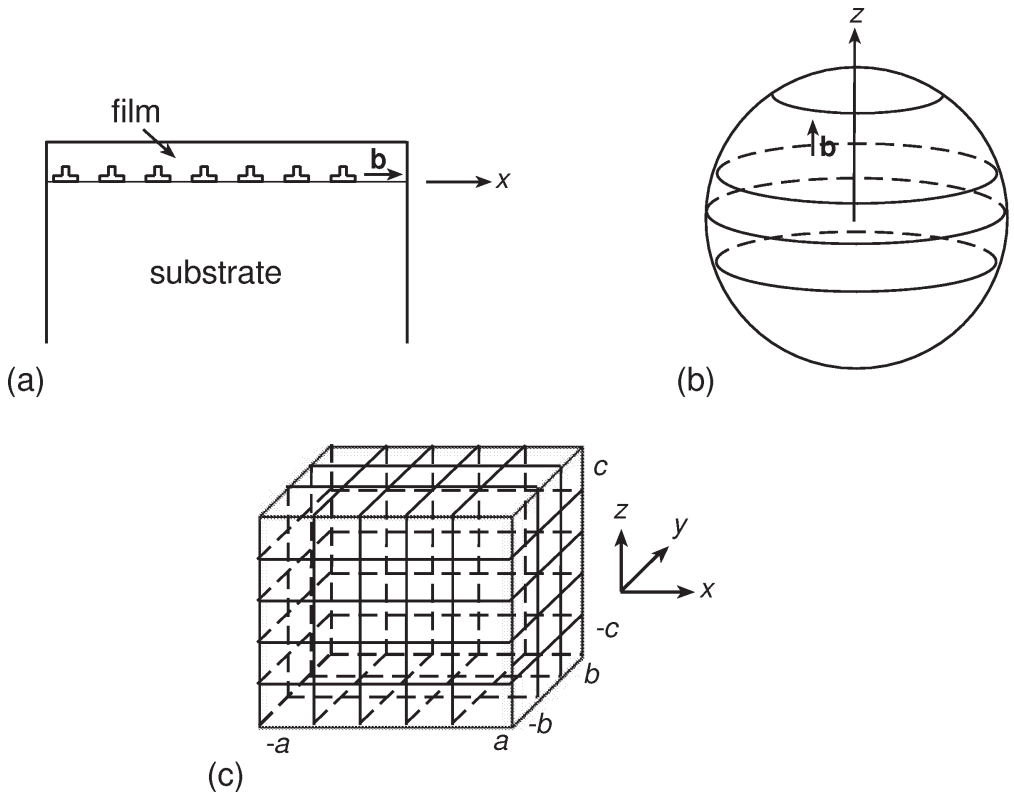

Fig. 3. Distributions of dislocations (a) and dislocation loops (b,c), which model the eigenstrains induced by a film on a substrate (a), spherical inclusion (b) and parallelepipedic inclusion (c).

$$\Phi_{xy} = -\ln(R_1 + \bar{z}),$$
$$\Phi_{xz} = -\ln(R_1 + \bar{y}),$$
$$\Phi_{yz} = -\ln(R_1 + \bar{x}), \qquad (29)$$

$C=\mu\varepsilon^*(1+\nu)/[2\pi(1-\nu)]$, $\bar{x} = x - x'$, $\bar{y} = y - y'$, $\bar{z} = z - z'$, $R_1^2 = \bar{x}^2 + \bar{y}^2 + \bar{z}^2$, and x_k, y_k, z_k (k=1,2) are the parallelepiped facet coordinates. For the parallelepiped shown in Fig. 3c, x_1=-a, x_2=a, y_1=-b, y_2=b, z_1=-c and z_2=c.

6. METHOD OF INFINITESIMAL INCLUSIONS

The methods of the Green functions and surface dislocation loops described in the previous sections are based on the construction of the solution for the inclusion elastic fields as the superposition of the known basic solutions. The same approach is used in the method of infinitesimal inclusions. In contrast to the methods of the Green functions and surface dislocation loops, where the basic solutions are those for the elastic fields of point forces, dislocations or dislocation loops, in the infinitesimal inclusion method the basic solutions are formed by infinitesimal inclusions. In this method, the displacements, strain and stress fields created by a real inclusion with a preset eigenstrain tensor are presented as the sum of the respective fields induced by infinitesimal inclusions with the same total eigenstrain tensor. If the inclusion eigenstrain is a pure dilatation, $\varepsilon^*_{ij}=\varepsilon^*\delta_{ij}$, the elastic fields of the inclusion of interest may be presented as the sum of the corresponding elastic fields created by dilatation center. Thus, the existing solutions for the dilatation centers in an isotropic infinite medium, half-space [85], two-phase mediums [100,101] and finite-thickness plate [111] provide an opportunity of obtaining the solutions for the elastic fields of inclusions with a purely dilatational eigenstrain, situated in such mediums. As an example, we write down the displacement field of a dilatation center in an isotropic half-space. Let the dilatation center be located at the point (x',y',z') of an isotropic half-space $z \geq 0$ (Fig. 4). Then the displacement field $\boldsymbol{u}^*(x,y,z)$ of this dilatation center follows as [85]

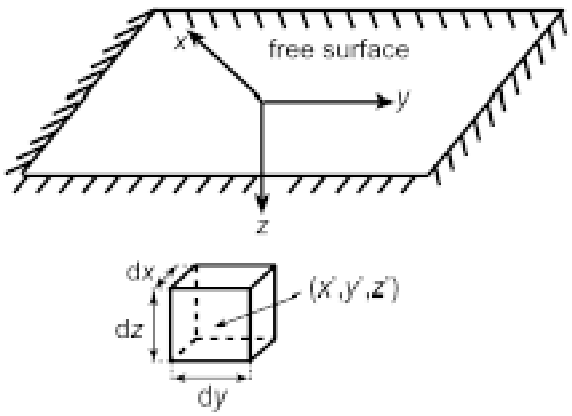

Fig. 4. Dilatation center in an isotropic half-space.

$$\boldsymbol{u}^*(x,y,z) = -P\left(\frac{\boldsymbol{R}_1}{R_1^3} + \frac{(3-4\nu)\boldsymbol{R}_2}{R_2^3} - \frac{6z\hat{z}\boldsymbol{R}_2}{R_2^5} - \frac{2\boldsymbol{e}_z}{R_2^3}\left[(3-4\nu)\hat{z} - z\right]\right). \quad (30)$$

In formula (30) $\boldsymbol{R}_1 = (\bar{x},\bar{y},\bar{z})$, $\boldsymbol{R}_2 = (\bar{x},\bar{y},\hat{z})$, $\bar{x} = x - x'$, $\bar{y} = y - y'$, $\bar{z} = z - z'$, $\hat{z} = z + z'$, $\boldsymbol{e}_z$ is the unit vector directed along the z-axis, $R_{1,2}^2 = \bar{x}^2 + \bar{y}^2 + (z \mp z')^2$, $A = (1+\nu)\varepsilon^* / [4\pi(1-\nu)]$, $P = A\,dx\,dy\,dz$, and dx, dy, dz is the volume of the dilatation center.

Formula (30) for the displacements created by a dilatation center in an isotropic semi-infinite solid has been used by Hu [93] for the calculation of the stresses induced by a parallelepipedic inclusion outside it. These stresses have been calculated by integration of the stress field of the dilatation center over the parallelepiped volume [93]. Afterwards, the expressions for the displacements and strains induced by such a parallelepipedic inclusion in an arbitrary point of a composite solid have been derived by Glas [94]. Glas also applied the solution obtained the calculation of the displacements and strains created in an isotropic semi-infinite solid by a truncated pyramid [35] and finite-length cylinder [41] with the dilatational eigenstrain $\varepsilon_{ij}^* = \varepsilon^* \delta_{ij}$ (Figs. 5a and 6a). For this purpose, the cylindrical and truncated pyramidal inclusions were modeled by a continuous distribution of parallelepipedic inclusions with an infinitesimal height and varying cross section (Figs. 5b and 6b). The displacements created by the pyramidal and cylindrical inclusions were then

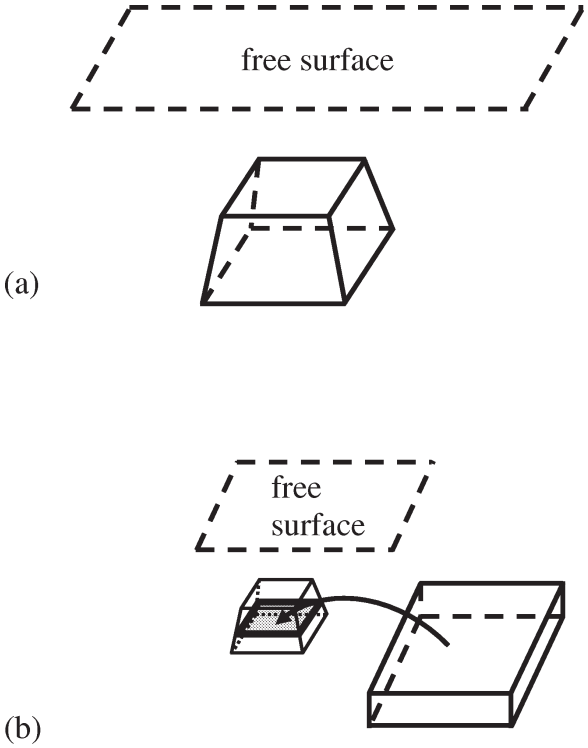

Fig.5. Truncated pyramidal inclusion in a semi-infinite composite solid (a) and its decomposition into parallelepipedic inclusion of infinitesimal height (b).

obtained through single integration of the displacements of the infinitesimal-height parallelepipedic inclusions. In general, the expressions for the displacements and total strains of the truncated pyramidal and finite-length cylindrical inclusions are very cumbersome. However, the solution for the cylindrical inclusion is considerably simplified if the cylinder length becomes infinite. In this case, the displacements u_i^c and total strains $\in_{ij}^c$ of the infinite cylindrical inclusion are as follows [41]:

$$u_x^c = Fx\left[-\left(\kappa_0 + \frac{4zz_{0+}}{Q_{1+}}\right)\frac{R^2}{Q_{1+}} + \Gamma^c(x,z) + \frac{R^2}{Q_{1-}}\bar{\Gamma}^c(x,z)\right], \quad (31a)$$

$$u_z^c = F\left[\left(\kappa_0 z_0 + \frac{2zQ_{2+}}{Q_{1+}}\right)\frac{R^2}{Q_{1+}} - z_{0-}\left(\Gamma^c(x,z) + \frac{R^2}{Q_{1-}}\bar{\Gamma}^c(x,z)\right)\right], \quad (31b)$$

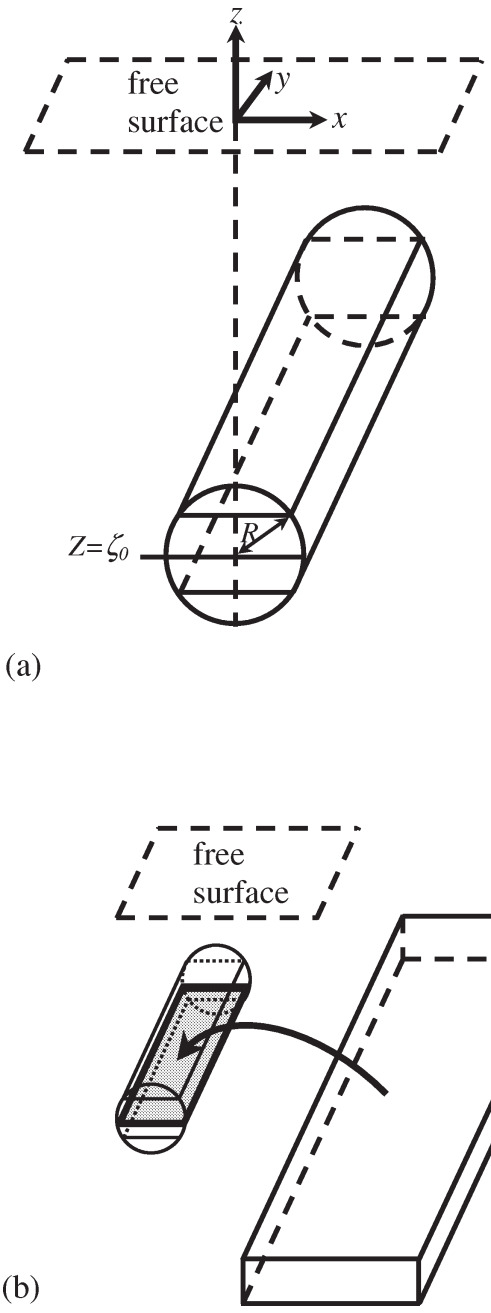

Fig. 6. Finite-height cylindrical inclusion in a semi-infinite composite solid (a) and its decomposition into parallelepipedic inclusion of infinitesimal height (b).

$$\epsilon^{c}_{xx}(x,z) = F\left[\frac{R^2}{Q_{1+}}\left(\kappa_0 Q_{2+} + \frac{4zz_{0+}(3x^2 - z_{0+}^2)}{Q_{1+}}\right) + \Gamma^{c}(x,z) - \frac{R^2 Q_{2-}}{Q_{1-}^2}\overline{\Gamma}^{c}(x,z)\right], \tag{32a}$$

$$\epsilon^{c}_{zz}(x,z) = F\left[\frac{R^2}{Q_{1+}}\left((\kappa_0 + 2)Q_{2+} - \frac{4zz_{0+}(3x^2 - z_{0+}^2)}{Q_{1+}}\right) + \Gamma^{c}(x,z) + \frac{R^2 Q_{2-}}{Q_{1-}^2}\overline{\Gamma}^{c}(x,z)\right], \tag{31b}$$

$$\epsilon^{c}_{xz}(x,z) = 2FR^2 x\left[-\frac{1}{Q_{1+}^2}\left(z_{0+} + \frac{2z(x^2 - 3z_{0+}^2)}{Q_{1+}}\right) + \frac{z_{0-}}{Q_{1-}^2}\overline{\Gamma}^{c}(x,z)\right], \tag{32c}$$

where R is the cylinder radius, (x=0, z=ζ_0) are the cylinder axis coordinates, $\kappa_0 = 4\nu\text{-}3$, F=(1+ν)ε*/[2(1-ν)], $z_{0\pm}$=$\zeta_0 \pm z$, $Q_{1\pm}$=$x^2 + z_{0\pm}^2$, $Q_{2\pm}$=$x^2 - z_{0\pm}^2$, $\overline{\Gamma}_c$=1 inside the cylinder and Γ_c=0 outside the cylinder, and Γ_c=1 - $\overline{\Gamma}_c$.

7. SUMMARY

In summary, we have provided a brief review of the solutions for the elastic fields of inclusions in composite solids and described the most popular analytical procedures for the calculation of the elastic fields of such inclusions: Green function method, surface dislocation method, the solution of equations of equilibrium, and infinitesimal inclusion method. We have shown that in spite of a small inclusion size in nanocomposites, their elastic fields may be effectively calculated using the methods of linear elasticity. The presence of a large number of solutions for the elastic fields of inclusions in composite solids with different geometrical and elastic characteristics gives an opportunity of studying the elastic behavior of a wide class of nanocomposites. At the same time, there are a few techniques that allow one to obtain new solutions for the elastic fields of nanoinclusions in nanocomposites on the basis of the existing basic solutions. The elastic fields acting in nanocomposites may also be calculated through a direct solution of boundary-value problems of the theory of elasticity.

ACKNOWLEDGEMENTS

This work was supported, in part, by the Office of US Naval Research (grant N00014-05-1-0217), INTAS (grant 03-51-3779), Russian Science Sup-

port Foundation, Ministry of Education and Science of Russian Federation, Russian Academy of Sciences Program 'Structural Mechanics of Materials and Construction Elements', and St. Petersburg Scientific Center.

REFERENCES

[1] D. Vollath and D.V. Szabo // *Adv. Eng. Mater.* **6** (2004) 117.
[2] S. Link and M.A. El-Sayed // *Annu. Rev. Phys. Chem.* **54** (2003) 331.
[3] S. Veprec // *Rev. Adv. Mater. Sci.* **5** (2003) 6.
[4] F. Yi-Si, Y. Ri-Sheng and Z. Li-De // *Chinese Phys. Lett.* **21** (2004) 1374.
[5] J. Bernholc, D. Brenner, M.B. Nardelli, V. Meunier and C. Roland // *Annu. Rev. Mater. Res.* **32** (2002) 347.
[6] N.N. Ledentsov and D. Bimberg // *J. Cryst. Growth* **255** (2003) 68.
[7] C. Teichert // *Phys. Rep.* **365** (2002) 335.
[8] V.A. Shchukin and D. Bimberg // *Rev. Mod. Phys.* **71** (1999) 1125.
[9] N.N. Ledentsov, V.M. Ustinov, V.A. Shchukin, P.S. Kop'ev, Zh.I. Alferov and D. Bimberg // Semiconductors **32** (1998) 343.
[10] W.L. Henstrom, C.-P. Liu, J.M. Gibson, T.I. Kamins and R.S. Williams // *Appl. Phys. Lett.* **77** (2000) 1623.
[11] X.Z. Liao, J. Zou, D.J.H. Cockayne, J. Qin, Z.M. Jiang, X. Wang and R. Leon // *Phys. Rev. B* **60** (1999) 15605.
[12] F. Boscherini, G. Capellini, L. Di Gaspare, F. Rosai, N. Motta and S. Mobilio // *Appl. Phys. Lett.* **76** (2000) 682.
[13] I. Kegel, T.H. Metzger, A. Lorke, J. Peisl, J. Stangl, G. Bauer, J.M. García and P.M. Petroff // *Phys. Rev. Lett.* **85** (2000) 1694.
[14] N. Liu, J. Tersoff, O. Baklenov, A.L. Holmes, Jr., and C.K. Shih // *Phys. Rev. Lett.* **84** (2000) 334.
[15] O.G. Schmidt and K. Eberl // *Phys. Rev. B* **61** (2000) 13721.
[16] G. Capellini, M. De Seta and F. Evangelisti // *Appl. Phys. Lett.* **78** (2001) 303.
[17] J.H. Seok and J.Y. Kim // *Appl. Phys. Lett.* **78** (2001) 3124.
[18] I. Kegel, T.H. Metzger, A. Lorke, J. Peisl, J. Stangl, G. Bauer, K. Nordlund, W.V. Schoenfeld and P.M. Petroff // *Phys. Rev. B* **63** (2001) 035318.
[19] X.Z. Liao, J. Zou, D.J.H. Cockayne, J. Wan, Z.M. Jiang, G. Jin and K.L. Wang // *Phys. Rev. B* **65** (2002) 153306.
[20] Ph. Sonnet and P.C. Kelires // *Phys. Rev. B* **66** (2002) 205307.
[21] Y. Zhang, M. Floyd, K.P. Driver, J. Drucker, P.A. Crozier and D.J. Smith // *Appl. Phys. Lett.* **80** (2002) 3623.
[22] M. Grundmann, O. Stier and D. Bimberg // *Phys. Rev. B* **52** (1995) 11969.
[23] Q. Xie, A. Madhukar, P. Chen and N.P. Kobyashi // *Phys. Rev. Lett.* **75** (1995) 2543.
[24] T. Benabbas, F. Francois, Y. Androussi and A. Lefebvre // *J. Appl. Phys.* **80** (1996) 2763.
[25] D.A. Faux, J.R. Downes and E.P. O'Reilly // *J. Appl. Phys*. **82** (1997) 3754.
[26] C. Pryor, J. Kim, L.W. Wang, A.J. Williamson and A. Zunger // *J. Appl. Phys*. **83** (1998) 2548.
[27] A.D. Andreev, J.R. Downes, D.A. Faux and E.P. O'Reilly // *J. Appl. Phys.* **86** (1999) 297.
[28] V. Holy, G. Springholz, M. Pinczolits and G. Bauer // *Phys. Rev. Lett.* **83** (1999) 356.
[29] G.S. Pearson and D.A. Faux // *J. Appl. Phys.* **88** (2000) 730.
[30] G. Springholz, M. Pinczolits, P. Mayer, V. Holy, G. Bauer, H.H. Kang and L. Salamanca-Riba // *Phys. Rev. Lett.* **84** (2000) 4669.
[31] G. Springholz, M. Pinczolits, V. Holy, S. Zerlauth, I. Vavra and G. Bauer // *Physica E* **9** (2001) 149.
[32] B. Jogai // *J. Appl. Phys*. **88** (2000) 5050.
[33] G. Muralidharan // *Jpn. J. Appl. Phys*., part 2, **39** (2000) L658.
[34] A.E. Romanov, G.E. Beltz, W.T. Fischer, P.M. Petroff and J.S. Speck // *J. Appl. Phys.* **89** (2001) 4523.
[35] F. Glas // *J. Appl. Phys*. **90** (2001) 3232.
[36] F. Glas // *Appl. Surf. Sci.* **388** (2002) 9.
[37] F. Glas // *Phil. Mag. A* **82** (2002) 2591.
[38] M. Tadić, F.M. Peeters, K.L. Janssens, M. Korkusiski and P. Hawrylak // *J. Appl. Phys.* **92** (2002) 5819.
[39] M. Tadić, F.M. Peeters and K.L. Janssens // *Phys. Rev. B* **65** (2002) 165333.
[40] B. Yang and E. Pan // *J. Appl. Phys.* **92** (2002) 3084.
[41] F. Glas // *Phys. Stat. Sol. (b)* **237** (2003) 599.
[42] C. Priester // *Phys. Rev. B* **63** (2001) 153303.
[43] H.X. Zhong, J.C. Wells, Q. Niu and Z.Y. Zhang // *Surf. Sci.* **539** (2003) L525.
[44] P. Liu, Y.W. Zhang and C. Lu // *Phys. Rev. B* **68** (2003) 195314.

[45] Q.X. Pei, C. Lu and Y.Y. Wang // *J. Appl. Phys.* **93** (2003) 1487.
[46] B. Yang and V.K. Tewary // *Phys. Rev. B* **68** (2003) 035301.
[47] V.M. Kaganer, B. Jenichen, G. Paris, K.H. Ploog, O. Konovalov, P. Mikulík and S. Arai // *Phys. Rev. B* **66** (2002) 035310.
[48] E. Bachlechner, A. Omeltchenko, A. Nakano, R.K. Kalia, I. Ebbsjö, A. Madhukar and P. Messina // *Appl. Phys. Lett.* **72** (1998) 1969.
[49] M.A. Cusack, P.R. Briddon and M. Jaros // *Phys. Rev. B* **56** (1997) 4047.
[50] O. Stier, M. Grundmann and D. Bimberg // *Phys. Rev. B* **59** (1999) 5688.
[51] L.-W. Wang, J. Kim and A. Zunger // *Phys. Rev. B* **59** (1999) 5678.
[52] Y. Kikuchi, H. Sugii and K. Shintani // *J. Appl. Phys.* **89** (2001) 1191.
[53] M.A. Makeev, W. Yu and A. Madhukar // *Phys. Rev. B* **68** (2003) 195301.
[54] M.A. Makeev and A. Madhukar // *Phys. Rev. B* **67** (2003) 073201.
[55] M.A. Makeev and A. Madhukar // *Phys. Rev. Lett.* **56** (2001) 5542.
[56] M.A. Migliorato, A.G. Cullis, M. Fearn and J.H. Jefferson // *Phys. Rev. B* **65** (2002) 115316.
[57] C. Kohler // *J. Phys.: Condens. Matter* **15** (2003) 133.
[58] A.V. Nenashev and A.V. Dvurechenskii // *JETP* **118** (2000) 497.
[59] T. Mura, *Micromechanics of Defects in Solids* (Martinus Nijhoff Publishers, Dordrecht-Boston-Lancaster, 1987).
[60] J.N. Goodier // *Phil. Mag.* **23** (1937) 1017.
[61] N.O. Miklestad // *J. Appl. Mech.* **9** (1942) A136.
[62] R.H. Edward // *J. Appl. Mech.* **18** (1951) 19.
[63] J.D. Eshelby // *Proc. R. Soc. London A* **241** (1957) 376.
[64] J.D. Eshelby // *Proc. R. Soc. London A* **252** (1959) 561.
[65] J.D. Eshelby, In: *Progress in Solid Mechanics*, Vol. 2, ed. by I.N. Sneddon and R. Hill (North-Holland, Amsterdam, 1961), p. 89.
[66] J. Eshelby, In: *Continuum theory of dislocations* (Inostrannaya Literatura, Moscow, 1963), in Russian.
[67] M.Yu. Gutkin and I.A. Ovid'ko // *Eur. Phys. J. B* **1** (1998) 429.
[68] N.A. Bert, A.L. Kolesnikova, A.E. Romanov and V.V. Chaldyshev // *Phys. Solid State* **44** (2002) 2240.
[69] L.Z. Wu and S.Y. Du // *Proc. R. Soc. London A* **455** (1999) 879.
[70] H. Hasegawa, V.G. Lee and T. Mura // *J. Appl. Mech.* **59** (1992) 107.
[71] W. Nowacki, *Thermoelasticity* (Pergamon, New York, 1962).
[72] V.I. Lawrenuk // *Izv. AN SSSR, Mechan. Tverd. Tela* N 3 (1979) 63, in Russian.
[73] Ya.S. Podstigach, V.A. Lomakin and Yu.M. Kolyano, *Thermoelasticity of Solids with Inhomogeneous Structure* (Nauka, Moscow, 1984), in Russian.
[74] S.L. Sass, T. Mura and J.B. Cohen // *Phil. Mag.* **16** (1967) 679.
[75] G. Faivre // *Phys. Stat. Sol.* **35** (1969) 249.
[76] R. Sankaran and C. Laird // *J. Mech. Phys. Solids* **24** (1976) 251.
[77] Y.P. Chiu // *J. Appl. Mech.* **44** (1977) 587.
[78] T.J. Gosling and J.R. Willis // *J. Appl. Phys.* **77** (1995) 5601.
[79] G.J. Rodin // *J. Mech. Phys. Solids* **44** (1996) 1977.
[80] J.R. Downes, D.A. Faux and E.P. O'Reilly // *J. Appl. Phys.* **81** (1997) 6700.
[81] H. Nozaki and M. Taya //*J. Appl. Mech.* **64** (1997) 495.
[82] T. Mura // *Mech. Res. Commun.* **24** (1997) 473.
[83] T. Mura // *Mater. Sci. Engng. A* **285** (2000) 224.
[84] H. Nozaki and N. Taya // *J. Appl. Mech.* **68** (2001) 441.
[85] R.D. Mindlin and D.H. Cheng // *J. Appl. Phys.* **21** (1950) 931.
[86] K. Aderogba // *Math. Proc. Camb. Phil. Soc.* **80** (1976) 555.
[87] K. Seo and T. Mura // *J. Appl. Mech.* **46** (1979) 568.
[88] H.Y. Yu and S.C. Sanday // *J. Appl. Mech.* **57** (1990) 74.
[89] A.A. Maradulin and R.F. Wallis // *Surf. Sci.* **91** (1980) 423.
[90] F. Loges, B. Michel and A. Christ // *Z. Angew. Math. Mech.* **83** (1985) 65.
[91] L.Z. Wu // *Acta Mech. Sinica* **19** (2003) 253.
[92] Y.P. Chiu // *J. Appl. Mech.* **45** (1978) 302.
[93] S.M. Hu // *J. Appl. Phys.* **66** (1989) 2741.
[94] F. Glas // *J. Appl. Phys.* **70** (1991) 3556.
[95] K.L. Malyshev, M.Yu. Gutkin, A.E. Romanov, A.A. Sitnikova and L.M. Sorokin // *Preprint of Ioffe Physico-technical Institute N 1109* (Leningrad, 1987), in Russian.

[96] M.Yu. Gutkin, I.A. Ovid'ko and A.G. Sheinerman // *J. Phys.: Condens. Matter* **15** (2003) 3539.
[97] H. Hasegawa, R.H. Liang and T. Mura // *J. Thermal Stresses* **15** (1992) 295.
[98] H. Hasegawa, V.G. Lee and T. Mura // *J. Appl. Mech.* **60** (1993) 33.
[99] L.Z. Wu and S.Y. Du // *J. Appl. Mech.* **63** (1996) 925.
[100] J. Dundurs and D.N. Guell // *Proc. 2nd South Western Conf. Theoret. and Appl. Mech. Devel. in Theoret. and Appl. Mech.* **2** (1965) 199.
[101] D.L. Guell and J. Dundurs // *Devel. in Theoret. and Appl. Mech*. **3** (1967) 105.
[102] K. Aderogba // *Phil. Mag* **35** (1977) 281.
[103] H.Y. Yu and S.C. Sanday // *Proc. R. Soc. London A* **434** (1991) 503.
[104] R.D. Mindlin // *Physics* **7** (1936) 195.
[105] H.Y. Yu and S.C. Sanday // *Proc. R. Soc. London A* **434** (1991) 521.
[106] L.J. Walpole // *J. Appl. Mech.* **59** (1997) 193.
[107] A.M. Korsunsky // *J. Appl. Mech.* **64** (1997) 697.
[108] C.Q. Ru, P. Schiavone and A. Mioduchowski // *Z. Angew. Math. Phys.* **52** (2001) 18.
[109] Y.F. Sun and Y.Z. Peng // *Appl. Math. Comput.* **140** (2003) 105.
[110] F. Kroupa and L. Lejcek // *Czech. J. Phys. B* **20** (1970) 1063.
[111] H.Y. Yu and S.C. Sunday // *Proc. R. Soc. London A* **438** (1992) 103.
[112] T. Chang, W. Guo and H.R. Dong // *J. Strain Anal. Eng.* **36** (2001) 277.
[113] M.Yu. Gutkin, I.A. Ovid'ko and A.G. Sheinerman // *J. Phys.: Condens. Matter* **12** (2000) 5391.
[114] M.A. Jaswon and R.D. Bhargava // *Proc. Camb. Phil. Soc.* **57** (1961) 669.
[115] R.D. List // *Proc. Camb. Phil. Soc.* **65** (1969) 823.
[116] J.R. Willis // *Q. J. Mech. Appl. Math.* **17** (1964) 157.
[117] R.D. Bhargava and H.C. Radhakrishna // *Proc. Camb. Phil. Soc.* **59** (1963) 821.
[118] R.D. Bhargava and H.C. Radhakrishna // *J. Phys. Soc. Japan* **19** (1964) 396.
[119] W.T. Chen // *Q. J. Mech. Appl. Math.* **20** (1967) 307.
[120] R.J. Asaro and D.M. Barnett // *J. Mech. Phys. Solids* **23** (1975) 77.
[121] I.A. Kunin and E.G. Sosnina // *Doklady AN SSSR* **199** (1971) 571, in Russian.
[122] H.C. Yang and Y.T. Chou // *J. Appl. Mech*. **43** (1976) 424.
[123] H.C. Yang and Y.T. Chou // *J. Appl. Mech*. **44** (1977) 437.
[124] R.A. Masumura and Y.T. Chou // *J. Appl. Mech.* **49** (1982) 52.
[125] H.T. Zhang and Y.T. Chou // *J. Appl. Mech.* **52** (1985) 87.
[126] C.Q. Ru // *Acta Mech.* **160** (2003) 219.
[127] E. Kröner, *Kontinuumstheorie der Versetzungen und Einenspannungen* (Springer, 1958).
[128] Lord Kelvin, In: *Mathematical and Physical Papers*, Vol. 1 (Cambridge University Press, 1882), p. 97.
[129] E. Mann, R. von Jan and A. Seeger // *Phys. Stat. Sol.* **1** (1961) 17.
[130] K.H.C. Lie and J.S. Koehler // *Adv. Phys.* **17** (1968) 421.
[131] H. Bross // *Phys. Stat. Sol.* **5** (1964) 329.
[132] D.M. Barnett // *Phys. Stat. Sol. (b)* **49** (1972) 741.
[133] J.W. Deutz and H.R. Schober // *Comp. Phys. Comm. (Netherlands)* **30** (1983) 87.
[134] S.A. Gunderson and J. Lothe // *Phys. Stat. Sol. (b)* **143** (1987) 73.
[135] C.Y.Wang and J.D. Achenbach // *Wave Motion* **18** (1993) 273.
[136] C.Y. Wang // *Int. J. Solids and Struct.* **31** (1994) 2591.
[137] Y. Hisada // *Bull. Seismolog. Soc. Am.* **85** (1995) 1525.
[138] T.C.T. Ting // *Q. J. Mech. Appl. Math.* **49** (1996) 1.
[139] T.C.T. Ting and V.G. Lee // *Q. J. Mech. Appl. Math.* **50** (1997) 407.
[140] E. Pan // *Appl. Math. Modell.* **21** (1997) 509.
[141] C.Y. Wang // *J. Eng. Math.* **32** (1997) 41.
[142] D.A. Faux and G.S. Pearson // *Phys. Rev. B* **62** (2000) R4798.
[143] E. Pan and F.G. Yuan // *Int. J. Solids Struct.* **37** (2000) 5329.
[144] V.K. Tewary // *J. Eng. Math.* **49** (2004) 289.
[145] K. Portz and A.A. Maradulin // *Phys. Rev. B* **16** (1977) 3535.
[146] K.P. Walker // *Proc. R. Soc. London A* **443** (1993) 367.
[147] E. Pan // *J. Appl. Mech.-Trans. ASME* **70** (2003) 101.
[148] L. Rongved // *Proc. 2nd Midwestern Conf. Solid Mech.*(1955) 1.

[149] J. Dundurs and M. Hetényi // *J. Appl. Mech.* **32** (1965) 671.
[150] V.A. Shchukin, D. Bimberg, V.G. Malyshkin and N.N. Ledentsov // *Phys. Rev. B* **57** (1998) 12262.
[151] S.P. Timoshenko and J.N. Goodier, *Theory of Elasticity* (McGraw-Hill, New York, 1970).
[152] A.G. Sheinerman and M.Yu. Gutkin // *Phys. Stat. Sol. (a)* **184** (2001) 485.
[153] I.A. Ovid'ko and A.G. Sheinerman // *Phil. Mag.* **84** (2004) 2103.
[154] M.Yu. Gutkin, V.R. Mirzoev, A.E. Romanov and M.K. Smagorinskii, In: *Physics of Strength of Heterogeneous Materials*, ed. by A.M. Leskovskii (Physiko-technical Institute Publ., Leningrad, 1988), p. 14, in Russian.